ROYAL SOCIETY
OF CHEMISTRY

PAPER

Check for updates

Pre-clinically evaluated visual lateral flow platform using influenza A and B nucleoprotein as a model and its potential applications†

Natpapas Wiriyachaiporn, [iD] *[a] Siriwan Sirikaew,[a] Nawakarn Chitchai,[ab] Pareena Janchompoo,[c] Weerakanya Maneeprakorn, [iD] [a] Suwussa Bamrungsap, [iD] [a] Ekawat Pasomsub[c] and Deanpen Japrung [iD] [a]

A visual colorimetric rapid screening system based on a lateral flow device for simultaneous detection and differentiation between influenza A and B nucleoprotein as a model was developed. Monoclonal antibodies, specific for either influenza A or B nucleoproteins, were evaluated for their reactivities and were used as targeting ligands. With the best antibody pairs selected, the system exhibited good specificity to both viruses without cross reactivity to other closely related respiratory viruses. Further semi-quantitative analysis using a strip reader revealed that the system is capable of detecting influenza A and B protein content as low as 0.04 and 1 ng per test, respectively, using a sample volume as low as 100 µL, within 10 minutes ($R^2 = 0.9652$ and 0.9718). With a performance comparison to the commercial tests, the system demonstrated a four-to-eight-fold higher sensitivity. Pre-clinical evaluation with 101 nasopharyngeal swabs reveals correlated results with a standard molecular approach, with 89% and 83% sensitivity towards influenza A and B viruses, and 100% specificity for both viruses.

Introduction

The recent coronavirus outbreak has brought to our attention the impact of acute respiratory tract infections. Of these respiratory pathogens, influenza remains one of the most highly contagious respiratory illnesses, affecting people of all ages worldwide. Despite being distinguished by seasonal epidemics, affecting 5–15% of the world population, occasional pandemic outbreaks usually take place every 10–15 years. This is due to the emergence of new strains caused by mutation of the strains circulating in the community.[1] It was reported that at least 3–5 million people have severe illnesses with complications and need further hospitalization, whilst there are approximately 250 000–500 000 deaths from influenza annually.[2] This raises an awareness of economical and health burdens caused by both epidemic and pandemic influenza outbreaks. In order to apply a preventive and effective treatment strategy, early diagnosis is urgently needed.[3]

Clinical diagnosis of respiratory illnesses based on clinical symptoms alone can be limited due to the overlapping symptoms of influenza-like illness (ILI) caused by different viral pathogens, including respiratory syncytial virus (RSV), rhinovirus, adenovirus, coronavirus, metapneumovirus, bocavirus, enterovirus, and parainfluenza virus.[3,4] To screen and diagnose patients with influenza virus infection, a number of different laboratory techniques, including conventional viral culture approach, molecular assays, serological method, immunofluorescence staining, and rapid antigen diagnostic tests, have been used.[5–7] Whilst viral culture and molecular assays provide the information regarding the identification of the outbreak strain and subtypes, serological method and immunofluorescence staining technique are useful for a detection and identification of antibodies to seasonal influenza viruses and the specific isolates. Although these techniques provide useful information, they are time-consuming techniques and their usefulness as a screening test often limited by the sophisticated step, expensive equipment, laboratory facilities, and expertise of the trained personnel.[8] To overcome these limitations, rapid testing can be more useful as a screening tool to prevent the seasonal episodes, control the outbreaks, and prepare for the next pandemic.

Of those technologies developed for a rapid pathogen detection *i.e.* isothermal nucleic acid amplification, microfluidic, three-dimensional nanostructured substrates, and mobile handheld technologies,[9–13] and lateral flow immunoassay, the latter technique has been used increasingly as POC and point-of-need applications,[14] especially in low-resource settings where laboratory facilities are limited.[15,16] These

[a]National Nanotechnology Center (NANOTEC), National Science and Technology Development Agency (NSTDA), PathumThani, 12120, Thailand. E-mail: natpapas@nanotec.or.th

[b]Faculty of Pharmacy, Thammasat University, Thailand

[c]Department of Pathology, Faculty of Medicine Ramathibodi Hospital, Mahidol University, Bangkok, Thailand

include the tests on biomarkers,[17] infectious agents,[18] and toxic compounds.[19–21] The main advantage of lateral flow technique is its simplicity, rapidity, and inexpensiveness. Within the system, different labels have been employed to facilitate the detection;[22] for example, including fluorescent-based system using fluorescent dyes/nanoparticles,[23] SERS-based system using anisotropic metal nanoparticles,[24] signal amplification-based system using enzyme as labels.[25] However, these systems have limitations in requiring additional steps and instruments, restraining their POC applications.[26] To achieve rapid screening purposes, simple system using gold nanoparticles (GNP) as labels has been extensively used for direct visual detection.[27,28]

Previously, rapid testing for screening respiratory pathogens, including influenza viruses, have been widely used. Differences in diagnostic sensitivity and specificity can be observed in difference assays. For example, Han *et al.*, reported the pooled sensitivity and specificity of 0.84 and 0.97, respectively, for such tests based on lateral flow immunoassay technique.[29] On the other hand, the tests can be valuable alternative method for a rapid screening due to its ease-of-use, rapidity, and applicability in POC applications. The test; therefore, can be helpful for diagnostic and treatment decision in clinical settings.[30–32]

Here, a visual colorimetric rapid screening system, based on lateral flow device for a simultaneous detection and differentiation between influenza A and B viruses as a model, was developed. To target the virus, influenza A and B nucleoproteins were selected as the target protein molecules. Of those influenza proteins, nucleoprotein is recognized as one of the most conserved proteins in the virus virion.[33,34] Using an in-house treatment and assembly of lateral flow strip test, the selection of targeting ligands, and the use of GNP as reporters, the system provides a ready-to-use platform for a direct visualization within 10 minutes, without the need of extra resources. The performance of the system is evaluated for its sensitivity and specificity, compared to that obtained from the available commercial tests. Subsequently, the system is pre-clinically evaluated with clinical specimens, correlated to molecular approach, to assess its application as an influenza screening tool. With the use of lateral flow device for detecting multiple targets, the system can be developed and applied as a rapid screening tool for respiratory illnesses caused by other pathogens.

Results and discussion

Verification of protein antigens and antibodies

Monoclonal antibody (mAb) to influenza A virus activity. To evaluate the activity of the mAbs in binding to their target protein, mAbs specific to influenza A and B viruses were assessed for their reactivity using sodium dodecyl sulfate–polyacrylamide gel electrophoresis (SDS–PAGE) and western blotting analyses. Proteins, including influenza A virus nucleoprotein, influenza B, RSV, adenovirus, and parainfluenza virus proteins, were loaded on the gel. After staining and destaining process, a clear distinct band at approximately 56 kDa and a band at 53 kDa, but with a lesser intensity, were observed in the lane loaded with influenza A nucleoprotein (Fig. S1A, lane 1, ESI†). Western blotting analysis revealed the presence of the

bands at 56 and 53 kDa, without cross reactivity to other virus proteins (Fig. S1B, lane 1, ESI†). This result indicates that the mAb is specific to influenza A nucleoprotein. The size of the protein at 56 kDa was shown to be correlated to the size of monomeric nucleoprotein. Whilst the size of monomeric influenza A nucleoprotein was reported to be 56 kDa, the truncated fragment at approximately 53 kDa as a result of proteolytic degradation of extracellular nucleoprotein has also been described earlier.[33–35]

mAb to influenza B virus activity. Similarly, mAb to influenza B virus was also evaluated in the same manner. SDS–PAGE analysis showed that there was a clear protein band present at 64 kDa, while other proteins having the size below 64 kDa can also be observed, although in a lesser extent (Fig. S1C, lane 1, ESI†). It should be noted that influenza B virus antigen was derived from inactivated Madin–Darby canine kidney (MDCK) cells infected with influenza B virus. As a result, other proteins with other sizes than that of 64 kDa could also be observed. However, western blotting analysis has showed only the presence of the protein at 64 kDa, without cross reactivity to other proteins (Fig. S1D, lane 1, ESI†). The size of the protein observed in the analysis was found to be matched with that of influenza B nucleoprotein at 64 kDa.[36] This result confirmed that the mAb reacted specifically to influenza B virus proteins, without cross reactivity to other virus proteins.

Principle of detection

Schematic diagram depicted in Fig. 1a illustrated the application of the developed system for screening influenza A and B antigens in one test. The components of the system, which consisted of sample application area, conjugate reservoir area, signal detection area, and absorbent pad was also illustrated in Fig. 1b. The principle integrates a specific recognition between the target antigen and the selected mAb pair, and a separation of the target molecules through the mean of chromatography. To enable a simple and direct visualization, GNP was used as reporter molecules. Within the device, a specific capture of influenza A and B virus antigens was achieved simultaneously through antibody–antigen complexation. As a sample migrated along the device, the target proteins were recognized by the GNP–mAb conjugates functioned as the detector probe. The complexes were then flowed and captured by the mAb immobilized on the test line (T-line) position of the reacting area. The excess conjugates were then flowed along the device and captured by the secondary antibody on the control line (C-line) position. The presence of both T-line and C-line signal indicated a positive result, meanwhile the presence of the C-line only can be referred to as negative result.

Characterization of the GNP–mAb conjugates

Monodispersed spherical GNP were synthesized and obtained. Transmission electron microscopy (TEM) and dynamic light scattering (DLS) analysis were used to characterize the particles. Fig. 2 reveals TEM images of the particles, demonstrating that the particles before and after conjugation to either mAb specific to influenza A or B virus were homogenously dispersed. Using
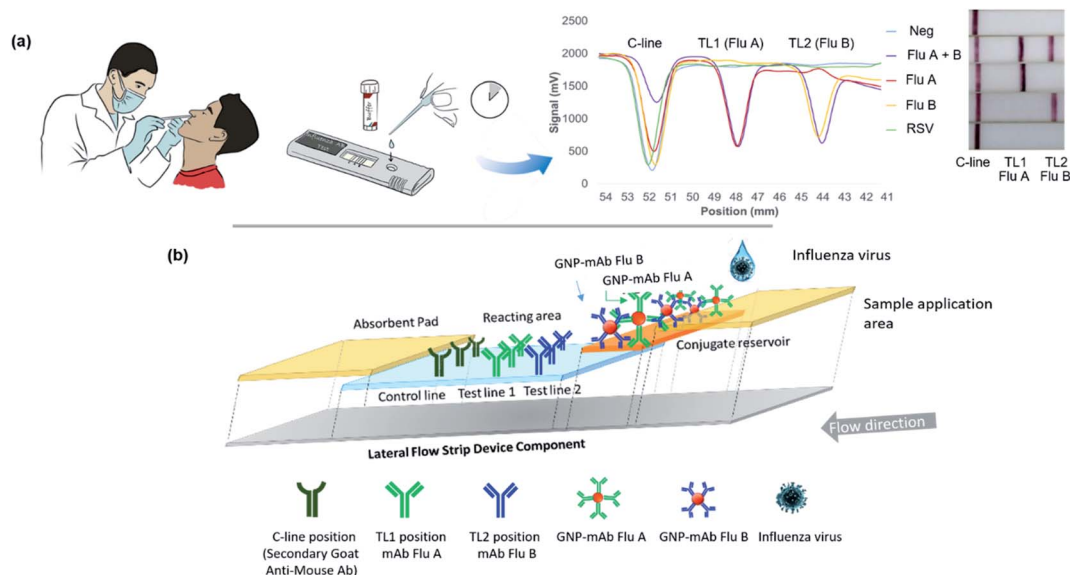
Fig. 1 Schematic diagram illustrated (a) the concept of the visual colorimetric rapid screening system based on lateral flow device for influenza A and B virus detection as a model. After sample collection, the sample was mixed with an analysis buffer before applied onto the device. The reaction was allowed to process, and the signal was visualized. The degree to which the formation of the complex at the test line position can be detected and quantified using the reader; (b) the components of the test system. Within the test, the virus proteins were recognized by the conjugates (GNP−mAb) and captured by the mAb on the test line position, enabling the detection signal. The presence of the control line indicates a validity of the test.

DLS analysis, it is also shown that the average hydrodynamic size of the plain particles was 24.0 ± 0.1 nm, whilst the size of particles after conjugated to mAb specific to influenza A and mAb specific to influenza B were 34.6 ± 0.9 nm and 44.4 ± 2.3 nm, respectively. DLS data for the size distribution of GNP before and after antibody conjugation were shown in Fig. S2, ESI.† To further characterize the particles, the zeta potential of the particles was determined. While the plain particles displayed a negative zeta potential of -33.9 ± 0.4 mV, the particles after conjugated to mAb specific to influenza A and mAb specific to influenza B exhibited -17.6 ± 0.6 mV and -20.1 ± 0.1 mV, respectively. The increased in the size and charge of the particles after conjugation suggested that the conjugation was successful.

Subsequently, the particles were characterized for the change in absorption spectrum. Fig. S3 (ESI†) showed the maximum of the absorption peak (A_{max}) at 526 nm of the plain particles. Further, the particles showed A_{max} at 532 and 534 nm after conjugated to mAb specific to influenza A and B, respectively. A small red-shift of the A_{max} indicated the successful of the conjugation. In the presence of high salt concentration, the conjugated particles were observed to be stable, as shown by an unchanged in colour. In contrast, the particles without the conjugation were shown to be aggregated, resulting in a change in color and a shift in A_{max} at 822 nm.

Performance of the system

Determination of limit of detection. With a direct visualization method, it was revealed that the system was capable to detect and distinguish between influenza A and B proteins,

without cross reactivity to negative sample containing buffer only and other tested respiratory virus proteins When the influenza A protein was used as a sample, the presence of the

	Distribution	Size (nm)	Charge (mV)
GNP		24.0 ± 0.1	-33.9 ± 0.4
GNP-mAb Flu A		34.6 ± 0.9	-17.6 ± 0.6
GNP-mAb Flu B		44.4 ± 2.3	-20.1 ± 0.1

Fig. 2 Characterization of the particles before and after mAb conjugation. TEM analysis revealed that the distribution of the particles before and after conjugation were monodispersed. The change in hydrodynamic size and charge of the particles after the conjugation was also confirmed using DLS analysis.

signal at the T-line position for influenza A (TL1) can be observed correctly, without cross reactivity to T-line for influenza B (TL2). Similarly, when influenza B protein used as a sample, the signal at TL2 and C-line position were observed, without the signal at TL1 position. In all cases, the signal at the C-line position was presence.

Further attempt to determine the limit of detection (LOD) for influenza A and B virus proteins was performed using influenza A and B proteins prepared in a 2-fold serial dilution ranged from 0–300 ng per test for influenza A protein and 0–8750 ng per test for influenza B protein, respectively. Fig. 3a shows the signal visualization at TL1 against influenza A protein concentration. Under optimal condition, it was showed that the TL1 signal decreased gradually when the protein was serially diluted until 0.04 ng per test (Fig. 3a). Similarly, the signal visualization upon the addition of influenza B proteins was also displayed with the limit of detection at 1 ng per test (Fig. 4a). In the absence of the target protein, only C-line signal was detected in both cases. In contrast, a high concentration of the target protein caused the formation of the sandwich immunocomplex between mAb–antigen, inducing the accumulation of GNP–mAb conjugates at the T-line. This subsequently enables direct signal visualization at the T-line position.

Subsequently to a direct visualization, semi-quantitative analysis using the reader was performed. Fig. 3b and 4b displayed the relationship between the target protein concentration and the relative signal response (RSR) for influenza A and B proteins, respectively. The linear relationship in the range of 0–1.2 ng per test ($R^2 = 0.9652$) for influenza A protein is demonstrated (Fig. 3b, inset figure). Similarly, the system also exhibited the linear relationship when the influenza B protein was added in the range of 0–546 ng per test ($R^2 = 0.9718$) (Fig. 4b, inset figure). The results showed that with a sample volume of
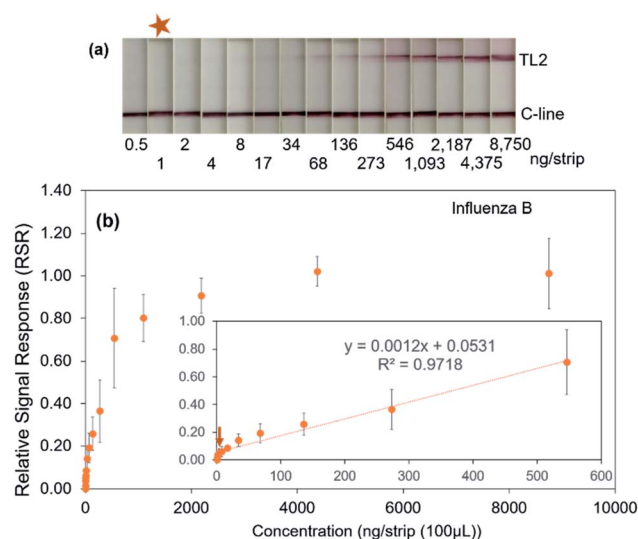

Fig. 4   (a) Result visualization and (b) the relative signal responses of the system against the presence of influenza B protein, ranged from 0–8750 ng per test. The increase in the signal was shown to be correlated to the increase of influenza B protein. Error bars were obtained from 3 separate experiments. Arrow and star indicate LOD.

100 µL, the system was able to detect influenza A and B proteins as low as 0.04 and 1 ng, respectively.

Specificity of the system. To assess the specificity of the system, other closely related respiratory virus proteins including RSV, adenovirus, and parainfluenza virus proteins, and other non-related proteins including avidin, c-reactive protein, hemoglobin, and insulin were included and used as a sample in the evaluation. Fig. 5 (inset figure) shows the signal visualization of the system containing influenza A and B
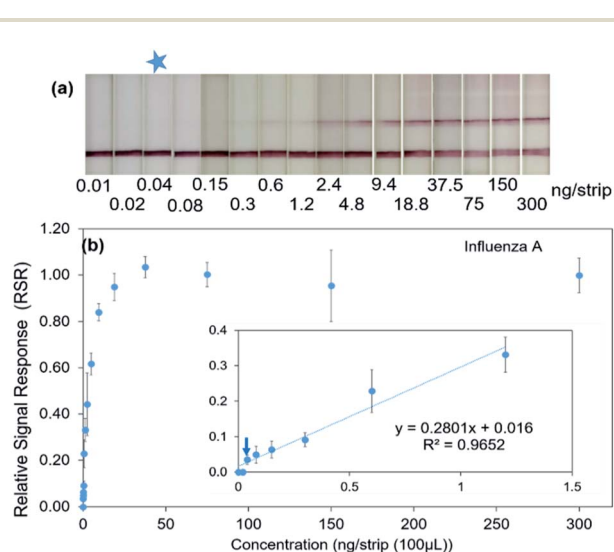

Fig. 3   (a) Result visualization and (b) the relative signal response against the presence of influenza A proteins, ranged from 0–300 ng per test. The increase in the signal was shown to be correlated to the increase of influenza A protein. Error bars were obtained from 3 separate experiments. Arrow and star indicate LOD.
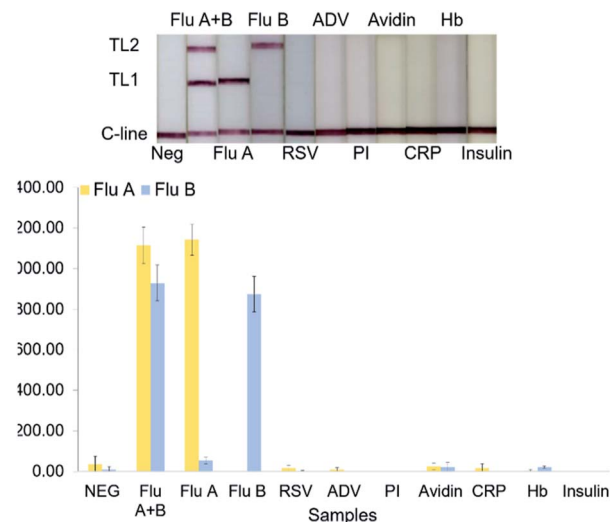

Fig. 5   Specificity of the system against different related respiratory viruses including influenza (Flu) A and B, RSV, adenovirus (ADV), parainfluenza (PI) virus, and other non-related proteins including avidin, CRP, haemoglobin (Hb) protein, and insulin. The presence of the signal at either TL1 or TL2 position, together with the C-line signal, indicates the positive result for influenza A and B virus, respectively.

viruses, other virus proteins, and other tested proteins. A high signal response value was also demonstrated when both influenza A and B protein antigens was added into the system (Fig. 5). In addition, in the system containing either influenza A or B proteins, a high signal response was also observed. In contrast, in the absence of influenza virus antigen (the negative control), no signal response was observed at both TL1 and TL2 position. It is also shown that other potentially related respiratory virus proteins and other non-related protein molecules showed no signal response at both T-line positions, suggesting that there was no significant interference from these tested virus proteins and molecules. This suggests that the system showed a good specificity towards influenza A and B viruses, without cross reactivity to the other tested virus proteins and molecules.

Comparison to the commercial tests. The performance of the system in detecting and differentiating influenza A and B protein antigens was subsequently compared to those of the two commercial rapid tests, which is routinely used in influenza screening. It was showed that the system was able to detect and distinguish between influenza A and B protein antigens correctly, in the same manner as the commercial tests. However, it was demonstrated that the developed system can detect influenza A protein antigen at 2-fold and 8-fold lower than that of commercial test 1 and 2, respectively, whilst the system is able to detect influenza B protein antigen at the same concentration with both commercial test 1 and 2 (Fig. S4 and S5, ESI†).

Pre-clinical evaluation of the system

Further to the performance evaluation of the system, 101 clinical specimens, including 44 influenza negative, 45 influenza A positive, 12 influenza B positive samples, were used to evaluate the performance of the system, as described previously. No signal was detectable in all influenza negative samples. Of those 45 influenza A positive samples, distinct signals at TL1 and C-line positions was observed in 40 samples, matched with those tested by commercial fluorescence-based rapid test. The other 5 samples revealed a weak TL1 signal, leading to a cut-off as a negative result. With this analysis, the sensitivity and specificity of the test for screening influenza A virus were reported to be 89% and 100%, with a positive predictive value (PPV), a negative predictive value (NPV), and percent accuracy were reported to be of 100%, 90%, and 94% (Table 1 and Fig. S6, ESI†).

With respect to influenza B positive samples, it was reported that 10 out of 12 influenza B positive samples showed correlated

results with those obtained from commercial fluorescent-based test and PCR method (molecular approach). The other two samples demonstrated weak TL2 signal, resulting in a negative result interpretation. This revealed the sensitivity and specificity of the developed tests for screening influenza B virus were reported to be 83% and 100%, respectively, while the PPV, NPV, and percent accuracy were reported to of 100%, 96%, and 96%, respectively (Table 1 and Fig. S6, ESI†).

It may be also worthwhile to further discuss the differences between the developed system and other systems. Previous studies reported different technologies used in detecting influenza virus. The most common technique used for influenza virus screening and detection is commonly shown to be molecular based approach, in which the technique is relied upon the amplification of the virus RNA. Regarding other rapid POC technologies, the technique is often integrated with other signal amplification technologies to enhance the sensitivity *i.e.* the use of gold nanoparticles, microfluidic chip, and fluorescent technologies.[37–39] Despite the high sensitivity, these technologies are laborious techniques and often require highly-trained personnel and instrument during analysis and result visualization processes. Particularly, they are still time-consuming methods. With respects to these factors, lateral flow platform offers advantages in its simplicity, and rapidity, and sensitive for a rapid POC screening purposes.

Experimental

Materials and reagents

Primary mouse monoclonal antibodies against influenza A nucleoprotein and influenza B nucleoprotein, secondary anti-mouse monoclonal with and without alkaline phosphatase enzyme (ALP) conjugation antibodies, and all respiratory virus protein antigens including recombinant influenza A nucleoprotein, influenza B virus-infected Madin–Darby Canine Kidney (MDCK) Cell lysate, RSV, parainfluenza virus, and adenovirus proteins were supplied from Fitzgerald, MA, USA, East Coast Bio, TN, USA, and Meridian Life Sciences, TN, USA, and Seracare (MA, USA). Forty-percent acrylamide/bis solution (29 : 1) was supplied from Bio-Rad Laboratories Inc. (CA, USA). Reagents used in sodium dodecyl sulfate–polyacrylamide gel electrophoresis (SDS–PAGE) and western blotting analyses including 5-bromo-4-chloro-3-indolyl phosphate (BCIP)/nitro blue tetrazolium (NBT), and device components were purchased from Merck Millipore (MA, USA). Bovine serum albumin (BSA), ammonium sulfate, β-mercaptoethanol, and coomassie brillant blue R250 solution were supplied from Sigma-Aldrich (MO, USA). All other chemicals and tested proteins were of analytical grade were supplied from Sigma-Aldrich (MO, USA), unless stated otherwise. Ultrapure water (18.25 MΩ cm) were obtained using Milli-Q system (Merck Millipore) and used throughout the experiments.

Clinical specimens

Clinical nasopharyngeal swab samples used in the evaluation were provided from Virology Unit, Department of Pathology,

Table 1 Pre-clinical evaluation of the system for a rapid screening of influenza A and B viruses using nasopharyngeal swabs, demonstrated by test system performance, including sensitivity, specificity, positive and negative predictive value, and accuracy, correlated to commercial rapid test and molecular approach

	Test system performance (%)				
	Sensitivity	Specificity	PPV	NPV	Accuracy
Influenza A	88.8	100	100	89.8	94.4
Influenza B	83.3	100	100	95.7	96.4

Faculty of Medicine, Ramathibodi Hospital, Bangkok, Thailand. After sample collection, the swabs were collected in the UTM™ transport medium (Copan Diagnostics, CA, USA). The samples were collected with full ethical approval granted by the University Ethics Committee. One hundred and one nasopharyngeal swab samples were collected from 101 patients, who had influenza-like illness symptoms. Of these 101 samples, 45 samples were diagnosed as influenza A virus positive, 12 samples were diagnosed as influenza B virus positive, and 44 samples were diagnosed as both influenza A and B virus negative using commercial fluorescent rapid test and molecular approach (PCR), as reference tests. Regarding molecular approach, samples were subjected to nucleic acid extraction and amplification using MagDeA® Dx SV (Precision System Science, Chiba, Japan) and RealStar® Influenza Screen & Type RT-PCR kit 4.0 (Altona-Diagnostics GmbH, Hamburg, Germany), respectively. Subsequent to the screening using the reference tests, the samples were immediately stored at $-80\ °C$ until further use.

Instruments

UV-Vis absorption spectra was recorded using a microplate reader (Power wave XS2, Bio-Tek, USA). Transmission electron microscopy (TEM) were taken on a JEM-2010 (JEOL, Japan). Surface charge of GNPs was determined by a Zetasizer (Malvern Instruments, UK). The CM4000 guillotine cutting module and the dispensing platform were obtained from BioDot (CA, USA). ESEQuant LR3 lateral flow device reader was obtained from Qiagen, Hilden, Germany.

Verification of protein antigens and antibodies

SDS–PAGE analysis. SDS–PAGE analysis was used to separate proteins as described previously.[40] The protein samples (10 μg) were mixed with loading buffer, containing 0.625 M β-mercaptoethanol, 1.36 M glycerol, 69.4 mM SDS, 0.02 mM bromophenol blue in 62.5 mM Tris buffer (pH 6.8), before preheated at 95 °C for 10 min for a preparation of electrophoresis. The proteins were separated using 15% (w/v) polyacrylamide gel with constant voltage at 100 V in a running buffer, containing 190 mM glycine and 3.48 mM SDS in 25 mM Tris buffer, pH 8.3 for 1.5 h. After staining and destaining, the gel was visualized and the image was record.

Western blotting analysis. Western blot analysis was performed as described previously with modification.[41] After electrophoresis, the proteins on the gel were transferred to a nitrocellulose membrane with constant voltage at 100 V in transfer buffer, containing 192 mM glycine and 20% (v/v) methanol in 25 mM Tris buffer (pH 8.3) for 1.5 h at RT. After washing and blocking step, the membrane was separately incubated with the dilution of their primary antibody, either mAb specific to influenza A or B viruses at optimal ratio at 4 °C for 16 h. Subsequently, the membrane was treated with secondary antibody (anti-mouse IgG, ALP conjugated) for 1 h, followed by re-rinsing step. A detection of protein bands was performed using BCIP/NBT substrate solution in the dark at RT until the color was developed. The reaction was stop by washing the membrane with distilled water and the image was recorded subsequently.

Gold nanoparticles synthesis

Gold nanoparticles (GNP) with the absorption maxima (A_{max}) at 526 nm was prepared by citrate reduction method according to a protocol described previously.[42] Briefly, 100 mL of 0.01% (w/v) tetrachloroauric acid was heated to reflux with continuous stirring, and 1 mL of 1% (w/v) trisodium citrate was rapidly added. The solution was boiled and stirred continuously until the color changed gradually from bright yellow to deep red. The reaction mixture was cooled and stored at 4 °C.

Preparation of GNP–mAb conjugates

The preparation of GNP–mAb conjugates was performed by using passive adsorption method and can be described in the following procedures. Briefly, the stock suspension of spherical GNP was homogenized in sonication bath before diluted to different folds with ultrapure water. Determination of the optimal conditions was achieved using the method, as described previously.[43] The mAb was conjugated to GNP to produce 'the detector probe'. For large scale conjugate production, the procedure was described as follows: briefly, a desired amount of mAb was mixed gently with 1 mL of GNP solution (optical density, O.D., at 542 nm (A_{max}) = 1.0). Under continuous gentle mixing, the mixture was left to react for 30 min at RT, followed by the addition of 10% (w/v) BSA in 20 mM borate buffer, pH 9. After incubation, the conjugates were then collected by centrifugation at $4400 \times g$ at 4 °C for 5 min before resuspending in 1% (w/v) BSA, in 20 mM borate buffer, pH 9. The final conjugates were then stored at 4 °C until used. In addition to TEM and DLS analysis, further characterization of the particles before and after conjugation was performed using induce particle aggregation method.[43,44]

Fabrication and assembly of the lateral flow device

Fabrication and the assembly of all the components of the lateral flow device can be illustrated as shown in Fig. 1. The device consists of four main components including sample application pad, conjugate reservoir pad, reacting nitrocellulose membrane, and absorbent pad, which are assembled together in a plastic housing cassette. To prepare the reacting membrane, mAb used a capture antibody and secondary anti-mouse antibody in a desired amount were dispensed onto the reacting membrane to form the test- and control lines, respectively, with a distance of 5 mm from each other. With multiplexed lateral flow device, the mAb specific to the influenza A proteins and the mAb specific to the influenza B proteins were dispensed with a distance of 5 mm from each other and were designated as TL1 and TL2, respectively. For conjugate reservoir pad preparation, a desired volume of the conjugates was loaded on the conjugate reservoir pad. For lateral flow device assembly, all components were assembly in a manner as depicted in Fig. 1, with the overlapping between each component of 2 mm.

Performance evaluation of the system and assay procedures

Qualitative analysis method using direct signal visualization. To evaluate the system performance for the detection of

the influenza A and B viruses, the serial two-fold dilutions of sample were prepared in a following procedure: the stock solution of the protein solution was prepared using 50 mM Tris–HCl buffer, pH 9 before diluted to different concentrations ranged from 0–3000 ng per test and 0–88 μg per test, for influenza A and B proteins, respectively. To perform the evaluation, the volume of 10 μL of each dilution was applied to the sample application window of the cassette, followed by an addition of 100 μL of the buffer containing 50 mM Tris–HCl buffer, pH 9. The reaction was allowed to react for 5 min before the signal at the T- and C-lines was visualized and recorded. The presence of both T- and C-line signal indicated the presence of the influenza proteins in the sample, while the presence of only C-line signal indicated the negative influenza protein detection. The performance evaluation of each dilution was performed in triplicate.

Semi-quantitative analysis using lateral flow device reader. Semi-quantitative analysis was performed using lateral flow device reader. After a direct signal visualization and image record, the test strip was inserted into a strip holder of the reader. The average value of the signal response, expressed as a peak height, at the T-line position (T_{av}) was determined and recorded at 10 min. The relative signal response (RSR) was calculated using the T_{av} value obtained from the sample containing the target influenza protein at various protein concentrations, compared with that obtained from the positive control (P_{av}). The RSR value calculation is demonstrated in the equation below. Each concentrations were obtained from three separate experiments. Either influenza A or B proteins at the concentration of 300 ng per test and 8750 ng per test was used as positive control in each case.

$$\text{RSR} = (T_{av})/(P_{av})$$

The specificity of the system was evaluated by using other respiratory virus proteins including either influenza A, influenza B, other respiratory viruses *i.e.*, RSV, parainfluenza, and adenovirus virus, and other non-related proteins *i.e.*, avidin, c-reactive protein, haemoglobin protein, and insulin proteins as samples. Assay procedure and the evaluation of specificity were performed in the same manner as described above.

Pre-clinical evaluation of the system

To evaluate the performance of the test system, nasopharyngeal swabs were used as the clinical specimens for evaluation. A total of 101 nasopharyngeal swabs, including 44 influenza virus negative samples, 45 influenza A virus positive samples, and 12 influenza B virus positive samples, were used as samples, as described previously. Prior to the sample application, the sample was mixed with an analysis buffer in a ratio of 1 : 1. Subsequently, a volume of 100 μL of the mixed sample was applied onto a sample application window of the device cassette and allowed to process before the signal was visualized directly at 5 min. The performance of the system was correlated to other methods including commercial rapid antigen detection test and molecular approach (Fig. S7, ESI†).

Pre-clinical evaluation of the test system performance was performed and correlated to those results obtained from commercial fluorescent-based test and molecular approach. To obtain sensitivity, specificity, positive and negative predictive values, and accuracy, true positive (TP), false negative (FN), true negative (TN), and false positive (FP) were used in the calculation as described previously[45,46] (Fig. S7, ESI†).

Conclusions

In summary, a visual colorimetric rapid screening system based on lateral flow device for influenza A and B virus detection and differentiation using nucleoprotein as target molecules has been designed and developed as a model. Under optimal condition, the system is capable to detect the target molecules at ng per test level, with a detection limit of 0.04 and 1 ng per test for influenza A and B proteins, respectively. With the integration of a reader, it is shown that the results obtained from visual colorimetric method and the semi-quantitative analysis are in good alignment. The system also showed selectivity for its target proteins against other closely related respiratory virus proteins and other non-related proteins. The performance of the system is shown to be 4- to 8-fold higher sensitive than commercial tests, using colorimetric detection. With correlation to reference methods based on commercial fluorescence-based test and molecular approach, the specificity of 100% and the sensitivity of 89% and 83% for influenza A and B viruses, respectively were demonstrated. The potential advantages of such visual colorimetric rapid screening system based on lateral flow device can be of great importance for other screening applications, including a detection and differentiation for other related infectious agents, toxins, and other contaminants.

Author contributions

Conceptualization: NW; Data curation: SS & NC; Formal analysis: NW, SS & NC; Funding acquisition: NW, WM & SB; Investigation: NW, SS, NC & PJ; Methodology: NW; Project administration: NW; Resources: NW, WM, SB, EP & DJ; Software: SS & NC; Supervision: NW; Validation: NW & SS; Visualization: NW & SS; Writing – original draft: NW; Writing – review & editing: NW.

Conflicts of interest

There are no conflicts to declare.

Acknowledgements

References

1 M. Jané, M. J. Vidal, N. Soldevila, A. Romero, A. Martínez, N. Torner, P. Godoy, C. Launes, C. Rius, M. A. Marcos and A. Dominguez, *Sci. Rep.*, 2019, **9**, 12853.

2 A. D. Iuliano, K. M. Roguski, H. H. Chang, D. J. Muscatello, R. Palekar, S. Tempia, C. Cohen, J. M. Gran, D. Schanzer, B. J. Cowling, P. Wu, J. Kyncl, L. W. Ang, M. Park, M. Redlberger-Fritz, H. Yu, L. Espenhain, A. Krishnan, G. Emukule, L. van Asten, S. Pereira da Silva, S. Aungkulanon, U. Buchholz, M. A. Widdowson, J. S. Bresee and Global Seasonal Influenza-associated Mortality Collaborator Network, *Lancet*, 2018, **391**, 1285–1300.

3 A. F. Dugas, A. Valsamakis, M. R. Atreya, K. Thind, P. A. Manchego, A. Faisal, C. A. Gaydos and R. E. Rothman, *Am. J. Emerg. Med.*, 2015, **33**, 770–775.

4 S. A. Call, M. A. Vollenweider, C. A. Hornung, D. L. Simel and W. P. McKinney, *JAMA, J. Am. Med. Assoc.*, 2005, **293**, 987–997.

5 K. A. Stellrecht, in *Diagnostic Molecular Pathology*, ed. B. C. William and J. T. Gregory, 2017, Molecular Testing for Respiratory Viruses, pp. 123–137, DOI: 10.1016/B978-0-12-800886-7.00011-X.

6 S. V. Vemula, J. Zhao, J. Liu, X. Wang, S. Biswas and I. Hewlett, *Viruses*, 2016, **8**, 96.

7 K. S. George, *Methods Mol. Biol.*, 2012, **865**, 53–69.

8 M. Petric, L. Comanor and C. A. Petti, *J. Infect. Dis.*, 2006, **194**, S98–S110.

9 H. Chen, A. Das, L. Bi, N. Choi, J. Moon, Y. Wu, S. Park and J. Choo, *Nanoscale*, 2020, **12**, 21560–21570.

10 H. Chen, S. Park, N. Choi, J. Moon, H. Dang, A. Das, S. Lee, D. Kim, L. Chen and J. Choo, *Biosens. Bioelectron.*, 2020, **167**, 112496.

11 H. Chen, K. Liu, Z. Li and P. Wang, *Clin. Chim. Acta*, 2019, **493**, 138–147.

12 Y. Xu, M. Liu, N. Kong and J. Liu, *Microchim. Acta*, 2016, **183**, 1521–1542.

13 X. Ding, M. G. Mauk, K. Yin, K. Kadimisetty and C. Liu, *Anal. Chem.*, 2019, **91**, 655–672.

14 W. C. Mak, V. Beni and A. P. F. Turner, *Trends Anal. Chem.*, 2016, **79**, 297–305.

15 O. Miočević, C. R. Cole, M. J. Laughlin, R. L. Buck, P. D. Slowey and E. A. Shirtcliff, *Front. Public Health*, 2017, **5**, 133.

16 H. Kim, D.-R. Chung and M. Kang, *Analyst*, 2019, **144**, 2460–2466.

17 X. Fu, J. Wen, J. Li, H. Lin, Y. Liu, X. Zhuang, C. Tian and L. Chen, *Nanoscale*, 2019, **11**, 15530.

18 X. Fu, Z. Cheng, J. Yu, P. Choo, L. Chen and J. Choo, *Biosens. Bioelectron.*, 2016, **78**, 530–537.

19 P. Tripathi, N. Upadhyay and S. Nara, *Crit. Rev. Food Sci.*, 2018, **58**, 1715–1734.

20 G. A. Posthuma-Trumpie, J. Korf and A. van Amerongen, *Anal. Bioanal. Chem.*, 2009, **393**, 569–582.

21 K. M. Koczula and A. Gallotta, *Essays Biochem.*, 2016, **60**, 111–120.

22 D. Quesada-González and A. Merkoçi, *Biosens. Bioelectron.*, 2015, **73**, 47–63.

23 S. Bamrungsap, C. Apiwat, W. Chantima, T. Dharakul and N. Wiriyachaiporn, *Microchim. Acta*, 2014, **181**, 223–230.

24 Y. Wang, J. Sun, Y. Hou, C. Zhang, D. Li, H. Li, M. Yang, C. Fan and B. Sun, *Biosens. Bioelectron.*, 2019, **141**, 111432.

25 C. Parolo, A. de la Escosura-Muñiz and A. Merkoçi, *Biosens. Bioelectron.*, 2013, **40**, 412–416.

26 E. Fu, T. Liang, J. Houghtaling, S. Ramachandran, S. A. Ramsay, B. Lutz and P. Yager, *Anal. Chem.*, 2011, **83**, 7941–7946.

27 N. Wiriyachaiporn, W. Maneeprakorn, C. Apiwat and T. Dharakul, *Microchim. Acta*, 2015, **182**, 85–93.

28 X. Huang, Z. P. Aguilar, H. Xu, W. Lai and Y. Xiong, *Biosens. Bioelectron.*, 2016, **75**, 166–180.

29 M. Han, T. Xie, J. Li, H. Chen, X. Yang and X. Guo, *BioMed Res. Int.*, 2020, **2020**, 3969868.

30 D. A. Green and K. StGeorge, *J. Clin. Microbiol.*, 2018, **56**, e00711–18.

31 Centers for Disease Control and Prevention, https://www.cdc.gov/flu/professionals/diagnosis/clinician_guidance_ridt.htm, accessed on April 24, 2021.

32 World Health Organization, http://apps.who.int/iris/bitstream/handle/10665/44304/9789241599283_eng.pdf;jsessionid=12044AD8127B58A34181F086DC1158B3?sequence=1, accessed on April 24, 2021.

33 Y. Hu, H. Sneyd, R. Dekant and J. Wang, *Curr. Top. Med. Chem.*, 2017, **17**, 2271–2285.

34 L. Sherry, M. Smith, S. Davidson and D. Jackson, *J. Virol.*, 2014, **88**, 12326–12338.

35 E. N. Prokudina, N. P. Semenova, V. M. Chumakov, I. A. Rudneva and S. S. Yamnikova, *Virus Res.*, 2001, 77, 43–49.

36 D. R. Londo, A. R. Davis and D. P. Nayak, *J. Virol.*, 1983, **47**, 642–648.

37 Y. Chi, Y. Ge, K. Zhao, B. Zou, B. Lin, X. Qi, Q. Bian, Z. Shi, F. Zhu, M. Zhou, L. Cui and C. Su, *Sci. Rep.*, 2017, 7, 44924, DOI: 10.1038/srep44924.

38 Y.-D. Maa, Y.-S. Chena and G.-W. Lee, *Sens. Actuators, B*, 2019, **296**, 126647.

39 B. Huang, N. P. West, J. Vider, A. J. Cox, T. Constantino, B. J. Harrower, A. T. Pyke, J. McMahon, J. A. Northill, T. Riordan and D. Warrilow, *Sci. Rep.*, 2017, 7, 18092.

40 U. K. Laemmli, *Nature*, 1970, **227**, 680–685.

41 T. Mahmood and P. C. Yang, *N. Am. J. Med. Sci.*, 2012, **4**, 429–434.

42 G. Fren, *Nat. Phys. Sci.*, 1973, **241**, 20–22.

43 S.-H. Paek, S.-H. Lee, J.-H. Cho and Y.-S. Kim, *Methods*, 2000, **22**, 53–60.

44 S. Christau, T. Moeller, J. Genzer, R. Koehler and R. von Klitzing, *Macromolecules*, 2017, **50**, 7333–7343.

45 A. Baratloo, M. Hosseini, A. Negida and G. El Ashal, *Emergency*, 2015, **3**, 48–49.

46 U.S. Food and Drug Administration, https://www.fda.gov/regulatory-information/search-fda-guidance-documents/statistical-guidance-reporting-results-studies-evaluating-diagnostic-tests-guidance-industry-and-fda, accessed on April 18, 2021.